Thermodynamic and Kinetic Study of the Eosin Dye Removal from Aqueous Solution by ZnO Nanoparticles

Amir Fadhil Dawood [*1], Ghalib Adris Atiya[2] and Donia Ahmed Abdulateef [1]**

[1]Department of Chemistry - College of Science - Diyala University
[2]Department of Chemistry - College of Education for Pure Science - Diyala University

[*]Dr_amer44@yahoo.com
[**]Ahmeddonia523@yahoo.com

Received: 29 December 2017 Accepted: 25 April 2018

Abstract

This research refers to the use of nanoparticles Zinc oxide (ZnO) in the removal of Eosin dye from aqueous solution by batch method. ZnO nanoparticles was characterized by using X-ray diffraction (XRD), Scanning electron microscopy (SEM), Atomic force microscope (AFM), Fourier transform infrared (FTIR) and the Brunauer–Emmett–Teller (BET) method. Optimum conditions for adsorption such as contact time, adsorbent dose, dye concentration, PH, and effect of temperature were studied. Contact time for the adsorption process was 2h. Adsorption isotherms been used to test the adsorption data (for Langmuir, Freundlich, Dubinin, Temkin) as it was fit to Freundlich isotherm. Thermodynamic functions data such as (ΔH°, ΔG°, ΔS°) of the adsorption process were calculated, which show the adsorption exothermic process and this process followed physisorption mechanism. Kinetic data were fit to pseudo- second order model.

Keywords: Adsorption, Eosin dye, Thermodynamics, Kinetic study of ZnO nanoparticles

DIYALA JOURNAL FOR PURE SCIENCES

Thermodynamic and Kinetic Study of the Eosin Dye Removal from Aqueous Solution by ZnO Nanoparticles

Amir Fadhil Dawood, Ghalib Adris Atiya and Donia Ahmed Abdulateef

دراسة ثرموديناميكية وحركية لإزالة صبغة الايوسين من المحاليل المائية بوساطة اوكسيد الخارصين النانوي

عامر فاضل داود[1] ، غالب ادريس عطية[2] و دنيا احمد عبد اللطيف[1]

[1]قسم الكيمياء – كلية العلوم – جامعة ديالى
[2]قسم الكيمياء – كلية التربية للعلوم للصرفة – جامعة ديالى

الخلاصة

في هذه الدراسة تم استخدام اوكسيد الخارصين النانوي في ازالة صبغة الايوسين من المحاليل المائية بطريقة الدفعة. وتم تشخيص اوكسيد الخارصين النانوي المحضر باستخدام تقنيات حيود الاشعة السينية (XRD)، المجهر الالكتروني الماسح (SEM)، مجهر القوة الذري (AFM) طيف الاشعة تحت الحمراء (FTIR) وطريقة المساحة السطحية (BET). تم دراسة الظروف المثلى للامتزاز مثل زمن الاتزان، ووزن السطح الماز، التركيز الاولي للصبغة، الدالة الحامضية و تأثير درجة الحرارة. تم التوصل الى زمن الاتزان لعملية الامتزاز في ساعتين. لاختبارقيم الامتزاز تم استخدام ايزوثرمات الامتزاز (لانكماير، فريندلج، دوبنين و تمكن) كان ايزوثيرم فريندلج الافضل. تم حساب قيم الدوال الثرموديناميكية لعملية الامتزازمثل ($\Delta H°, \Delta G°, \Delta S°$) والتي تظهر ان عملية الامتزاز باعثة للحرارة وتتبع هذه العملية الية الامتزاز الفيزيائي. القيم الحركية تكون ملائمة للمرتبة الثانية الكاذبة مع معامل ارتباط عالي($0.99R^2$).

الكلمات المفتاحية : الامتزاز، صبغة الايوسين، دراسة ثرموداينميكية، دراسة حركية اوكسيد الخارصين النانوي.

Introduction

Dyes are widely used in industries such as textile, leather; food and plastic materials [1]. The wastewater after the dyeing process carries the residual and unspent dye substances which are usually discharged into the environment as such without being treated. This discharged effluent is toxic in nature, imparts color to the receiving water or soil and interferes with both land and aquatic plant and animal life [2]. The most dyes are stable to light and oxidizing agents in nature [3]. Various methods such as biodegradation [4], advanced oxidation [5], ultrafiltration [6] and adsorption [7] have been applied to remove dyes from aqueous solutions. Adsorption has gained increased attention in removing dyes because its simplicity,

high efficiency, minimization of chemical sludge, and regeneration of adsorbents. A wide variety of adsorbents, have been used for the removal of dyes from aqueous solutions including activated carbon, zeolite [8], perlite [9], chitin [10], lemon peel [11], graphene oxide [12] etc.

Experimental

Instruments

UV-Visible (Shimadzu, Japan 1700) was used to measure the dye concentration in aqueous solution. The pH of all solutions was recorded by pH meter (7110 (wtw), Germany). The temperature was controlled using isothermal water bath shaker (BS-11, Korea). ZnO characterized using XRD (Shimadzu company (Japan) (XRD-6000)) with Cu kα radiation (λ = 0.15406nm), the measurements conditions of XRD are 40kv, 30mA, the scanning range is 20 - 80° and the scanning speed 5 deg/min. FTIR (Shimadzu (IR PRESTIGE 21) with KBr pellet technique. The effective range was from 4000 to 400cm^{-1}, AFM (SPM-AA3000, Advanced Angstrom Inc.), SEM (Type Tescan), BET (Q-surf 9600 (USA)).

Preparation zinc oxide nanoparticles

Zinc oxide (ZnO) nanoparticles were prepared by precipitation method. The Zinc nitrate solution (Zn $(NO_3)_2.6H_2O$) (0.2 M) was placed in (2000 ml) beaker placed on a hot plate magnetic stirrer. A magnetic bar is used in order to obtain homogeneous mixing of the material. The two electrodes of PH meter were inserted in the solution. Measure and monitor the pH value of the solution during the slowly addition of the sodium bicarbonate solution ($NaHCO_3$) (0.4 M) from burette. The temperature of the solution was fixed at 80°C. The addition continued until the pH of the solution reaches (6.8) where the precipitation was completed. After the completion of reaction, the precipitate is allowed to settle overnight. It is then filtered off and the precipitate is washed several times with distilled water, until free from excess bicarbonate which may be present then dried the precipitates at 70-80 °C for 2 hour and then calcined at 400 °C for 3 hours in an oven to obtain the ZnO nanoparticles.

Preparation of Standard Solutions for Eosin dye

The dye concentration of (250 mg/L) was prepared by dissolving (0.025g) in volumetric flask (1000 ml) of distilled water. Solutions of different concentrations (2 - 20) mg/L were prepared by dilutions from the standard solution and the solutions are left for 24 hours in order to homogenize. Dilute (0.1 M) HCl and (0.1 M) NaOH was used for PH adjustment. The UV-Visible spectrometer used to determination calibration curve for eosin dye at λ_{max} (516nm). The dye adsorption by batch process to study different parameter such as contact time (10-140) min, dose of adsorbent (ZnO) (0.01-0.09g), PH (1-10), temperature (20-40°C). The samples were shaken and kept in a thermostat for (2h) ,the samples were then filtered in a centrifuge for 15 min (at 3500 rpm) and then filtered again and analyzed spectrophotometrically. The percentage dye adsorption from the aqueous solution was determined according to the following equation (% Adsorption) [13]:

$$\% \textbf{ Adsorption} = \frac{C_o - C_e}{C_o} \times 100 \qquad (1)$$

Where C_o and C_e (both mg/L), are the initial concentration and the concentration at any time respectively. The adsorption capacity Q_e (mg/g).

$$Q_e = \frac{C_o - C_e}{m} . V_{sol.} \qquad (2)$$

Q_e: Amount of solute adsorbed per unit weight of adsorbent (mg/g).

C_e: Equilibrium concentration of solute (mg/L). $V_{sol.}$: Volume of solution (L). m: mass of adsorbent (g).

Results and Discussions

Characterization of ZnO Nanoparticles

FTIR spectra of ZnO nanoparticles are shown in Figure (1). Metal oxides generally give absorption bands in fingerprint region i.e. below 1000 cm^{-1} arising from inter-atomic vibrations. The peak observed at 3446.79 cm^{-1} may be due to O-H stretching assigned to the water adsorption on the metal surface. The peak at 1651.07 cm^{-1} is correspond to Zn-O

stretching, the peaks at 669.68 and 545.85 cm^{-1} are correspond to deformation vibration. The metal – oxygen frequencies observed for the respective metal oxides are in accordance with literature values [14].

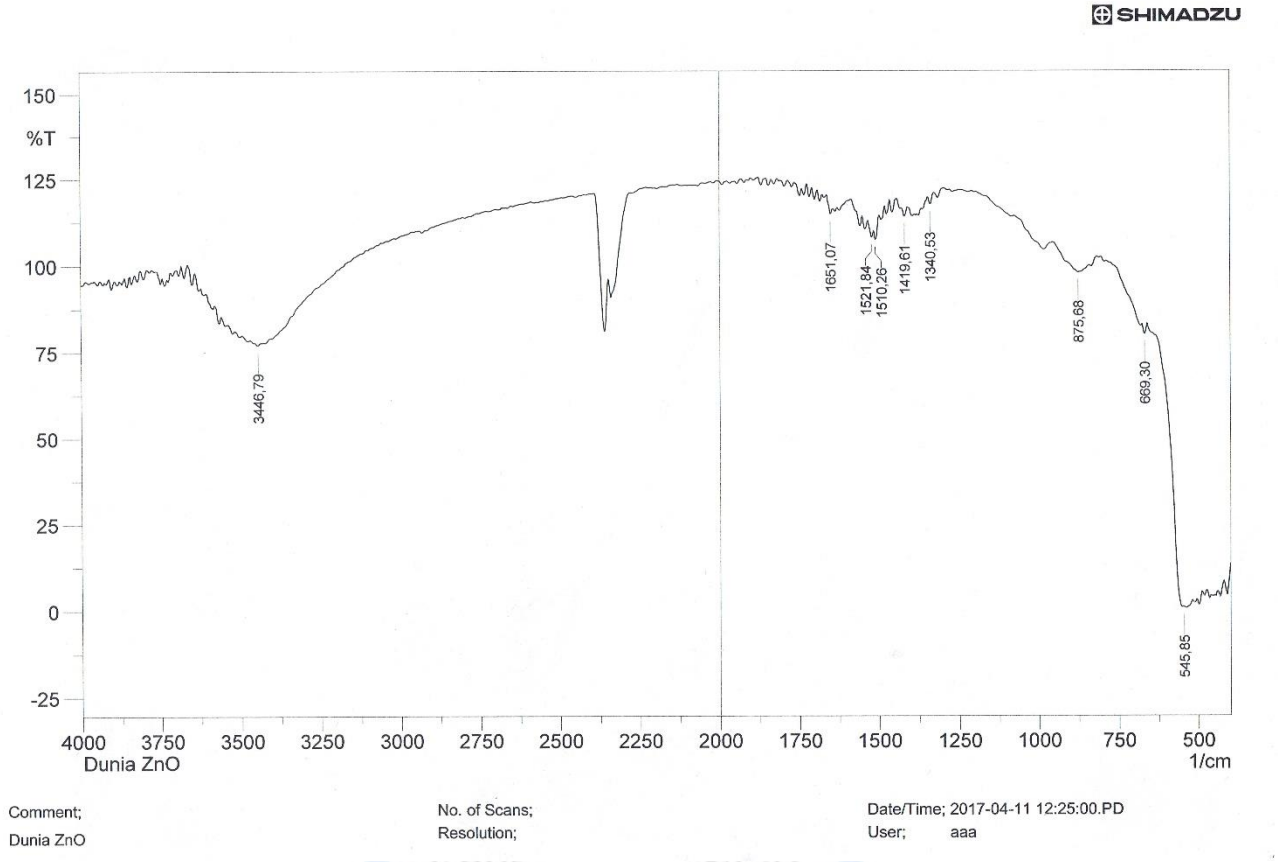

Figure 1: FTIR spectrum of ZnO nanoparticles

X-ray diffraction (XRD)

Figure (2) shows diffraction peaks around the 2Θ angles of 31.77° (100), 34.42° (002) and 36.25° (101) belong to hexagonal wurtzite system. The crystal parameters are (a = 3.249Å and c= 5.206 Å).All diffraction data are in good agreement with JCPDS files **No. 36-1451**, no other phases are detected, and the diffraction peaks are sharp and the crystal grows completely with high purity.

Thermodynamic and Kinetic Study of the Eosin Dye Removal from Aqueous Solution by ZnO Nanoparticles

Amir Fadhil Dawood, Ghalib Adris Atiya and Donia Ahmed Abdulateef

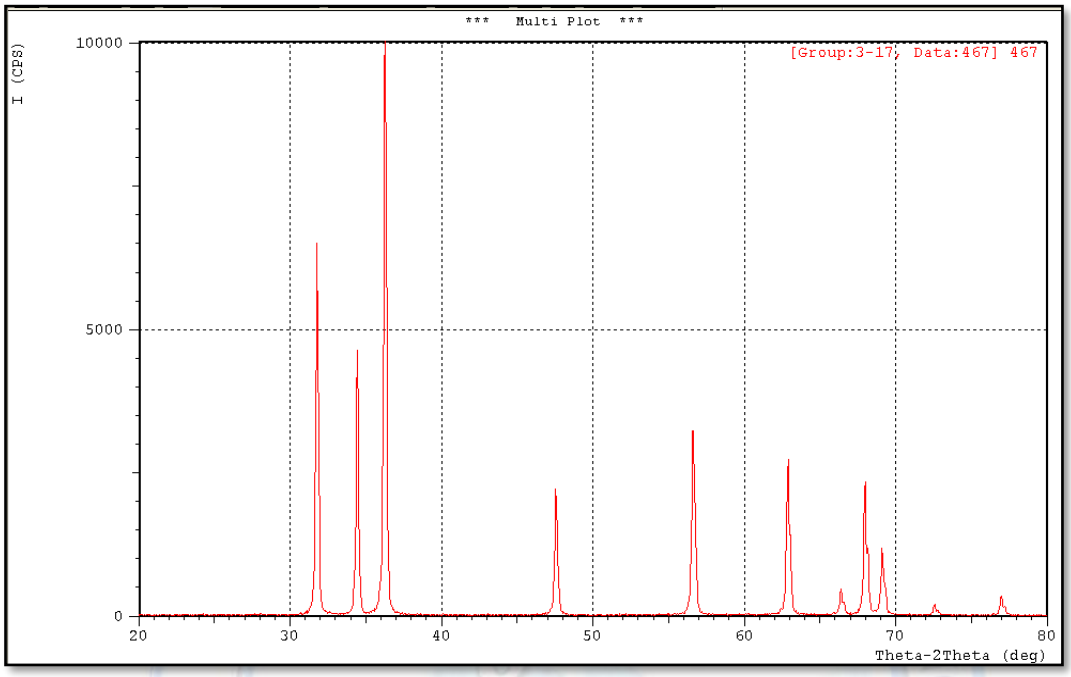

Figure 2: XRD pattern of ZnO nanoparticles

It is very clear that the major reflections between (2Θ =30°–40°) indicate more crystalline regions in the ZnO sample, also the less intense peaks at 48°, 57°, 63° and 67° (2Θ values). The detailed analysis of the XRD and the assignments of various reflections are given in the Table (1).

Table 1: Strongest three peaks in XRD of ZnO nanoparticles

No.	Peak No.	2Θ (deg)	d(Å)	FWHM (deg)	Intensity (counts)
1	3	36.2942	2.47321	0.18160	4543
2	1	31.8134	2.81058	0.19020	2635
3	2	34.4619	2.60040	0.17650	1899

Particle size has been estimated by using Debye-Scherer's Equation

$$D = 0.9\lambda / \beta \cos \Theta \quad (3)$$

Where D: crystallite size, **:λ** wave length (0.154nm), **β**: full width at half maximum, Θ: diffraction angle, D = 47.8 nm calcined at 400 °C [15].

The surface area (BET)

The specific surface area of adsorbents surfaces should be determined if any physical chemical interpretation of its behavior as an adsorbent is to be possible. The properties of surface area were provided through the adsorption of nitrogen at 77 K which is the temperature equilibrium between the vapor and liquid phase. The results of surface area for the (ZnO) nanoparticles are 6.706 m^2/g.

Scanning electron microscopy analysis (SEM)

The SEM images of the ZnO nanoparticles sample that prepare by precipitation method are shown in Figure (3). In Figure (3) shown a homogeneous distribution with bigger agglomerates results in lack of coagulation of particles, and existence of some voids along the deposited layer. From SEM images it is confirmed that the particles having size (100-150) nm.

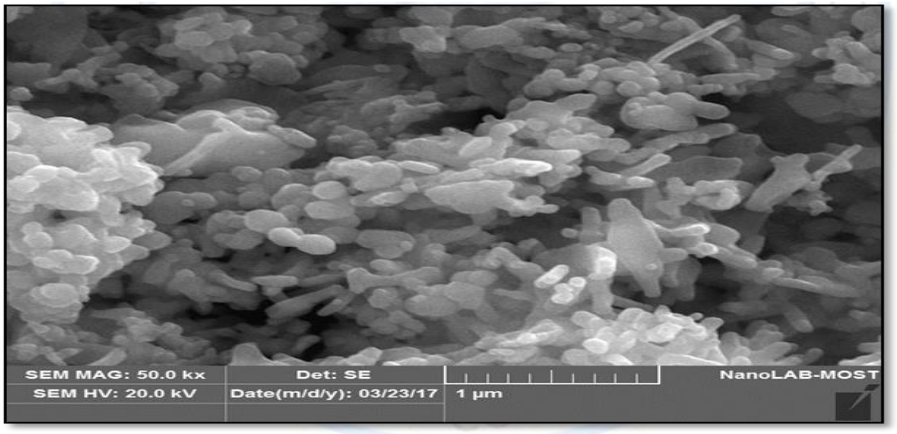

Figure 3: SEM image of ZnO nanoparticles.

Atomic Force Microscopy (AFM)

Atomic force microscopy (AFM) is a powerful characterization tool for determination the particle size and surface organization of the synthesized materials. The wet ability of a surface is dependent on its chemical composition, and also on the topography of the surfaces. (ZnO) nanoparticles are characterized by AFM image in two and three-dimensional and particles sizes distributions for adsorbent surface was represented in Figures (4, 5). They show that the average diameter of the particle was (139 nm) for ZnO [16].

Thermodynamic and Kinetic Study of the Eosin Dye Removal from Aqueous Solution by ZnO Nanoparticles

Amir Fadhil Dawood, Ghalib Adris Atiya and Donia Ahmed Abdulateef

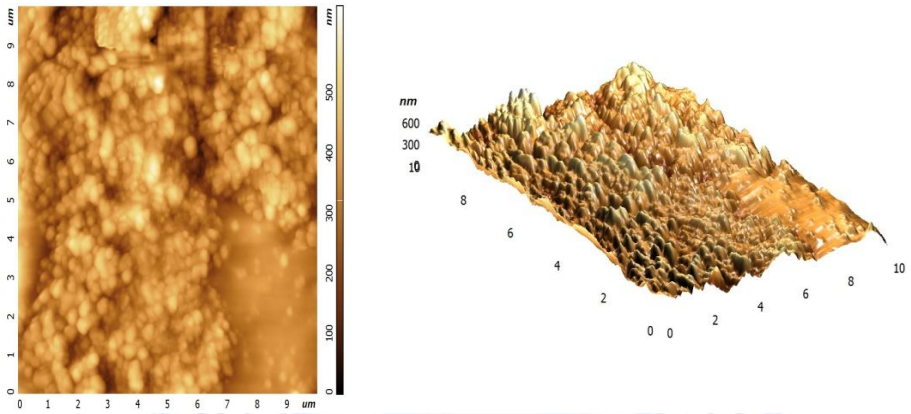

Figure 4: AFM images of ZnO nanoparticles

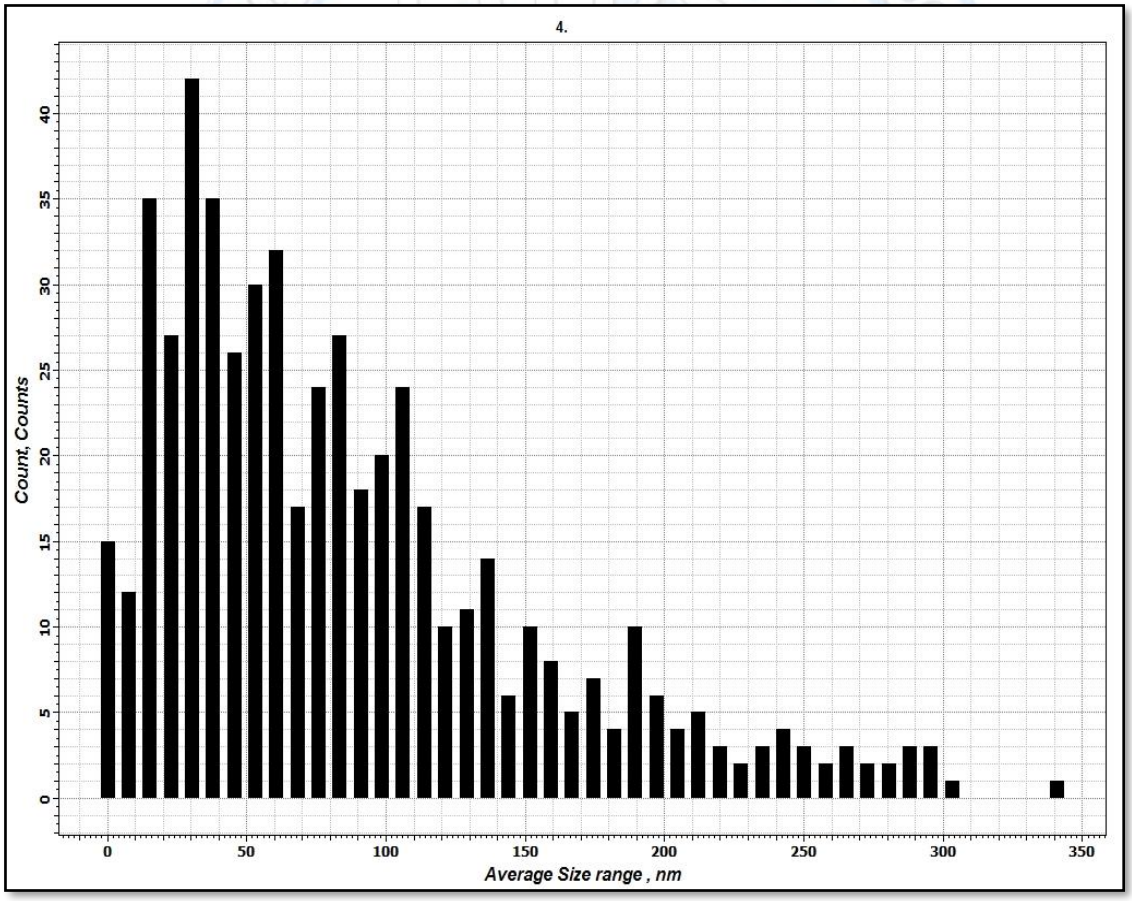

Figure 5: Particle size distribution of ZnO nanoparticles

Optimum conditions for adsorption

Determination of Equilibrium Time of adsorption

Series adsorption experiments in (10-150) min of contact time range were performed and the data were shown in Fig.6. The adsorption rate of dye gradually increased with the increase of contact time from 10 to 120 min and then remained constant [17], with further increase in contact time; therefore, a period of 120 min of equilibrium was selected for the next studies. In the initial stage, dye contact quickly with a lot of available active sites on the surface of ZnO, resulting in the occurrence of the fast adsorption with increase of the contact time, the available active sites gradually lessened and the driving force weakened, leading to the slow adsorption process and taking long time to achieve adsorption equilibrium.

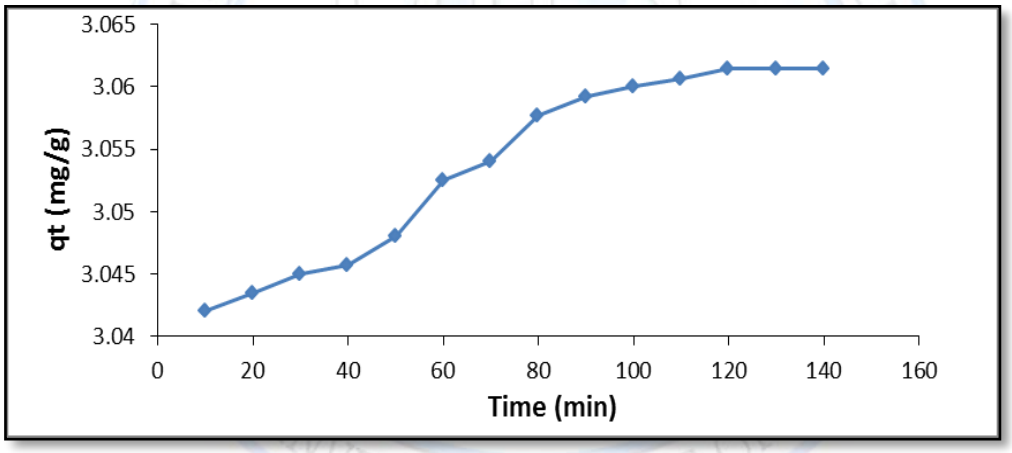

Figure 6: Effect of equilibrium time for adsorption of Eosin dye on (ZnO) nanoparticles at (25 ^{o}C, C_o= 30 ml of 10 ppm, dose 0.04 g and pH=7).

Adsorbent Weight

The effect of adsorbent on percentage removal of dye was examined by taking different quantities of ZnO ranging from 0.01 to 0.09 gm. Our results showed in Figure (7), which the best removal efficiency was obtained at 0.04gm [18].

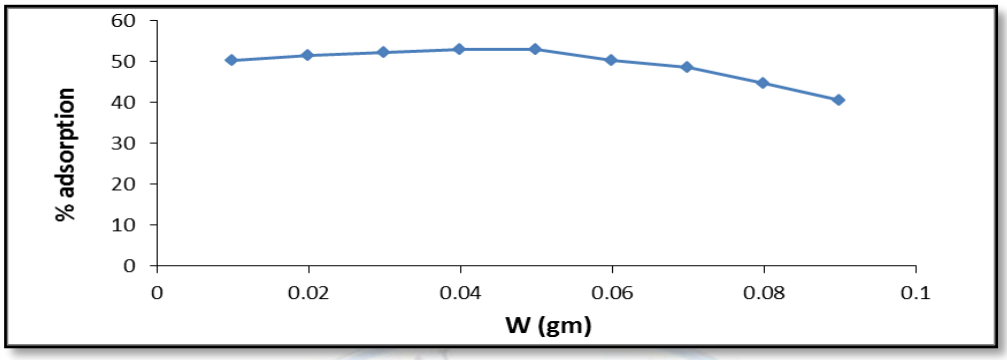

Figure 7: Effect of adsorbents weight on the adsorption of Eosin dye on (ZnO) nanoparticles at (25 ^{o}C, C_o=30ml of 10 mg/L and pH=7).

Effect the concentration of dye on adsorption

Figure (8) shows that the effect concentration of dye on percentage removal of dye by taking different quantities of dye ranging from (2 -20) mg/L. Our results showed in figure (8), that the best adsorption efficiency was obtained at 10 mg/L [19].

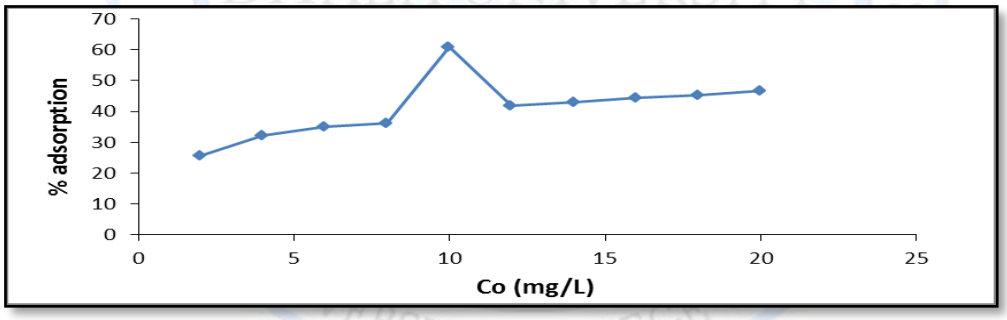

Figure 8: Effect of dye concentration on adsorption of Eosin dye on (ZnO) nanoparticles at (25 ^{o}C, dose 0.04gm and pH =7)

Effect of pH

The initial pH of the eosin dye solution can significantly affect the adsorption capacity of the dye because it affects the charge distribution of the surface of the adsorbent (ZnO) as well as adsorbate (the dye molecules). Figure (9) shows that in acidic medium the adsorption capacity is maximum and decreases with the increase pH and according to the following pH = 4> 7> 9.

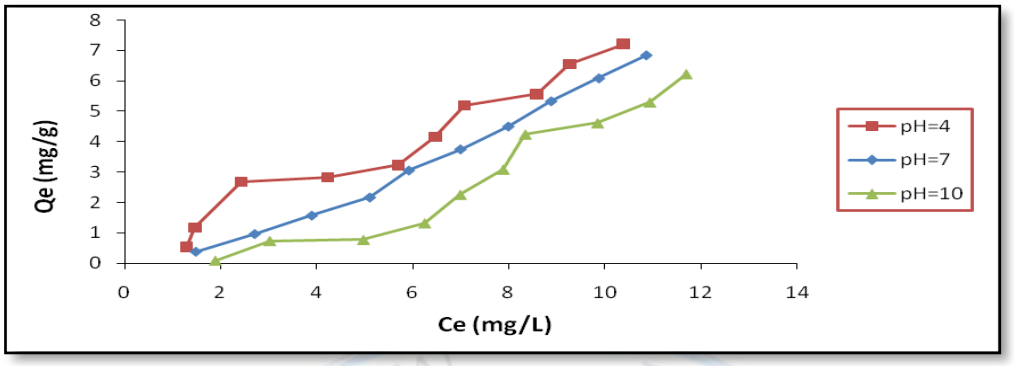

Figure 9: Effect of pH on the adsorption of Eosin dye on ZnO nanoparticles at (25ºC. 30ml of 10 mg/L dye and dose 0.04gm).

Adsorption Kinetics

Both pseudo first order and pseudo second order kinetics were applied to the adsorption data [20].

$$\ln (q_e - q_t) = \ln q_e - k_1 t \quad (4)$$

$$t / q_t = 1/ k_2 q_e^2 + (1/ q_e) t \quad (5)$$

Where q_e and q_t (mg/g) are the amounts of dye adsorbed at equilibrium and time t respectively, k_1 and k_2 are the rate constant of pseudo first order (min^{-1}) and pseudo second order (g/mg. min). The plots of the equations were examined for best fit by comparing their correlation coefficients (R^2). Figures (10 and 11) shown the straight plots of ln (q_e- q_t) vs .t and t / q_t vs.t, respectively. The correlation coefficients of the linear curves of both kinetics shows that the process more likely follows a second order kinetics. Pseudo-second order model assumes that the rate –limiting step involves chemisorption of adsorbate on the adsorbent [21]. The adsorption rate constant for each model was shown in Table (2). The kinetics data were well fitted by the pseudo-second order, as demonstrated by the higher regression coefficient (R^2) obtained. In addition, the calculated q_e values for the pseudo-second order is highly matched with the experimental data as compared with those of the pseudo-first order model. This indicated that the adsorption kinetics of dye on ZnO was not diffusion controlled [22].

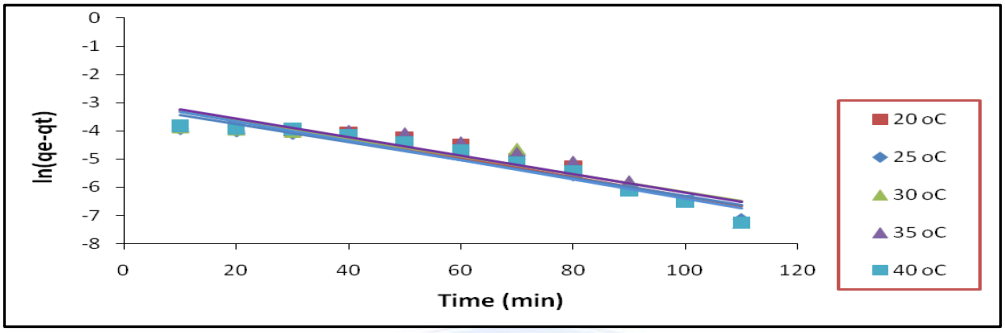

Figure 10: plot of pseudo-first order model of Eosin dye on ZnO nanoparticles

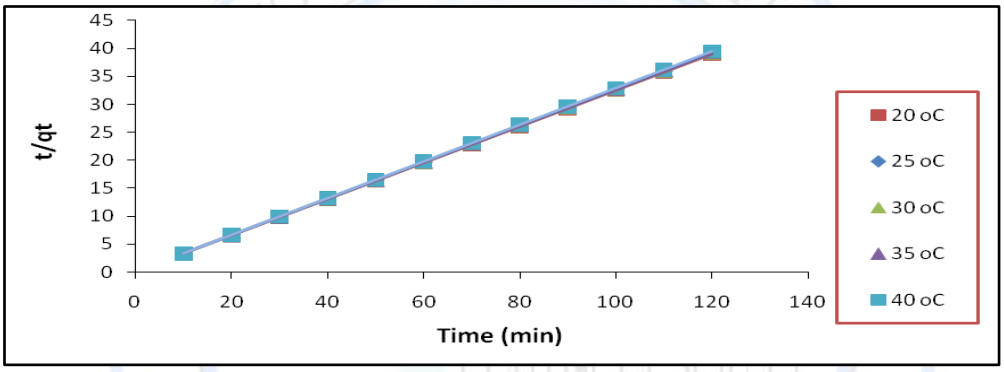

Figure 11: plot of pseudo –second order model of eosin dye on ZnO nanoparticles

Table 2: Kinetics parameters for adsorption of Eosin dye on ZnO nanoparticles

	T (C°)	qe (.exp)	pseudo-first- order			second pseudo-order			
			q_e (calc)	K_1 min^{-1}	R^2	qe (.calc)	K_2 $gmg^{-1}min^{-1}$	H	R^2
C_o mg/L10	20	3.074	0.053	0.033	0.897	3.078	1.529	14.411	1
	25	3.061	0.044	0.032	0.906	3.065	1.715	16.113	1
	30	3.054	0.049	0.031	0.852	3.058	1.555	14.543	1
	35	3.050	0.054	0.032	0.861	3.054	1.459	13.615	1
	40	3.039	0.049	0.034	0.930	3.043	1.644	15.230	1

Isotherm adsorption

The adsorption isotherms are to explore the relation between the adsorbate concentration in the bulk (at equilibrium) and the amount adsorbed at the surface. In this study four commonly used isotherm models (Langmuir, Freundlich, Temkin, and Dubinin-Kaganer-Radushkevich) were applied to the experimental data to explain the dye –nanoZnO interaction. The Langmuir

isotherm model assume monolayer coverage of the adsorbate over a homogenous adsorbent surface with identical adsorptions sites and their binding energies and neglecting any interactions between adsorbed ions, atoms or molecules [23] with each molecule adsorbed onto the surface having the same adsorption energy. The Langmuir isotherm is expressed as [24]:

$$\frac{C_e}{Q_e} = \frac{1}{q_{max} k_L} + \frac{C_e}{q_{max}} \quad \textbf{(6)}$$

Where C_e is the equilibrium concentration of dye (mg/L), q_{max}, Q_e are the maximum adsorption capacity corresponding to complete monolayer coverage on the surface (mg/g) and capacity at equilibrium (mg/g) respectively and K_L is Langmuir constant (L/mg) [25] related to energy of sorption. Therefore, a plot of C_e/Q_e versus Ce gives a straight line of slope $1/q_{max}$ and intercept ($1/ K_L q_{max}$). From the intercept and slope of the plots in Figure (12). The values of q_{max} and K_L were listed in Table (4). Table (4) shows that the values of q_{max} and K_L are decreased when the solution temperature increased from 20 to 40°C, indicates that the dye is favorably removed at lower temperatures, which shows that the adsorption process is exothermic. A dimensionless constant separation factor of Langmuir isotherm (R_L) was also calculated using equation [26].

$$\mathbf{R_L = 1/ (1+K_L C_o)} \quad \textbf{(7)}$$

C_o is the initial concentration of Eosin dye solution (mg/L) and K_L (L/mg) is the Langmuir adsorption constant given in Table (3). Table (3) explains the relation between R_L and the natural of adsorption and table (4) shows that the values of R_L are <1.

Table 3: Values of R_L and type of isotherm.

Value of R_L	> 1 L R	L = 1 R	$R_L < 1$	L = 0R
Type of isotherm	Unfavorable	Linear	Favorable	Irreversible

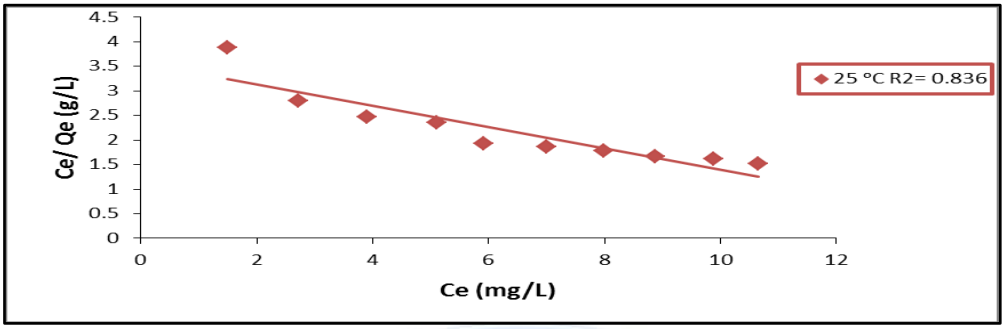

Figure 12: Isotherm Langmuir for Eosin dyes on ZnO nanoparticles at 25 °C.

The Frenudlich model is a case for multilayer adsorption and adsorption on heterogeneous surface energies and it gives an exponential distribution of active sites. The linear form of this model is represented by:

$$\ln Q_e = \ln K_F + 1/n \ln C_e \quad (8)$$

The Frenudlich constants K_F and n, which respectively indicating the adsorption capacity and the adsorption intensity are calculated from the intercept and slope of plot ln Q_e versus ln C_e respectively, as shown in Figure (13). The intensity of adsorption (n) showed low values (n<1); this indicates a very low affinity between adsorbents and adsorbate. The Freundlich constant (K_F) decreases with increasing the temperature and this indication for exothermic reaction. The values of n are larger than 1, which represents a favorable removal condition [27].

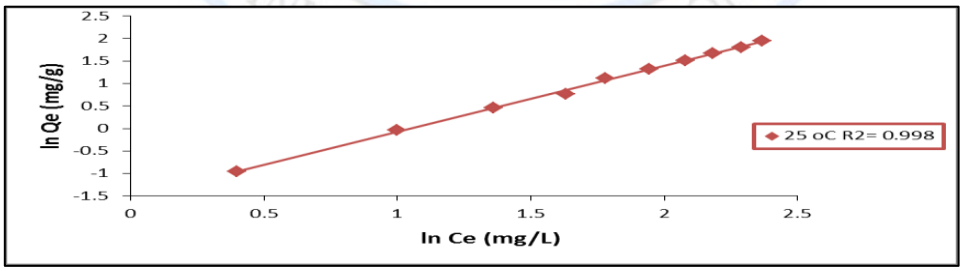

Figure 13: Isotherm Freundlich for Eosin dyes at different concentrations and 25 °C on ZnO

A more common isotherm than Langmuir is the Dubinin-Kaganer –Radushkevich (DKR) model was proposed by Dubinin which does not assume a homogenous surface of surface of sorbent. It is applied to determine the adsorption mechanism (physical or chemical). The linear form of (DKR) as follows [28]:

$$\mathbf{lnQ_e = lnq_{max} - \beta\varepsilon^2} \quad \textbf{(9)}$$

Where q_{max} is the maximum sorption capacity (mg/g), **β**is the activity coefficient related to mean sorption energy (mol^2/ J^2), and **ε** is the Polanyi potential defined as:

$$\varepsilon = \mathbf{RT\ ln\ (1+\ 1/C_e)} \quad \textbf{(10)}$$

Where R is the gas constant (kJ/mol. K). The slope of the plot of lnqe versus ε^2 gives β and the intercept yields the sorption capacity q_{max}, as shown in Figure (14). Prognostication of the adsorption mechanism (physical or chemical sorption) can be done by calculating the value of the mean sorption energy, E (J/mol) from the relation [29].

$$\boldsymbol{E} = (-\mathbf{2\ \beta})\ -\mathbf{0.5} \quad \textbf{(11)}$$

The values of β, q_{max}, E and R^2 as a function of temperature are listed in Table (4). If the values of E were less than 8 kJ/mol, the mechanism maybe a physical adsorption, While E values between 8-16 kJ/mol assumes the adsorption to be controlled by ion exchange and E greater than 16kJ/mol presume a particle diffusion mechanism (chemical process). It can be observed that the values of E may be physical (electrostatic) in nature.

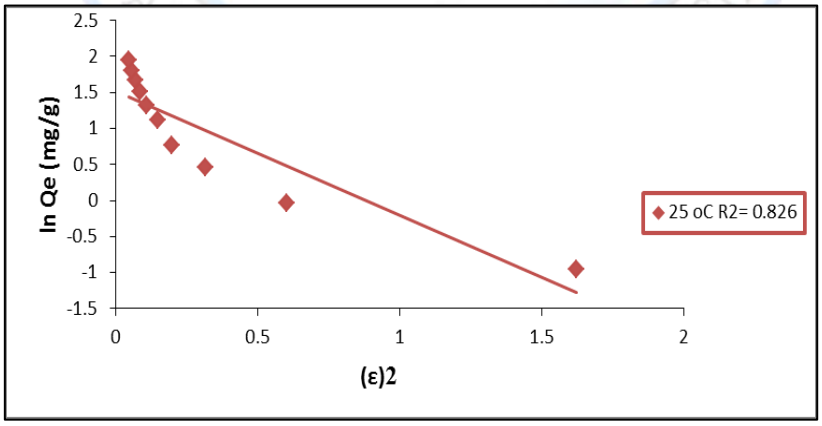

Figure14: Isotherm Dubinin (DKR) for Eosin dye at 25 ºC and different concentrations on ZnO

The Temkin isotherm in the linear form has been used as the following:

$$\mathbf{Q_e = BlnK_T + BlnC_e} \quad \textbf{(12)}$$

Where B= RT/ b is related to heat of adsorption (J/mol), K_T is equilibrium binding constant (L/gm), R is the gas constant (8.314 J/mol. K). Both K_T and B are calculated (as shown in Table (4)) from the intercept and the slope of curve between lnCe and Qe as in Figure (15).

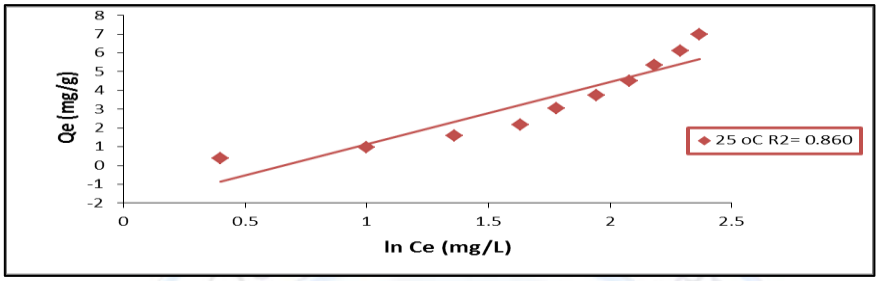

Figure15: Isotherm Temkin for Eosin dye at 25 °C and different concentrations on ZnO.

Table4: The calculated adsorption parameters of the four used isotherms

	Langmuir				Freundlich		
(C°) T	K_L	R^2	q_{max}	R_L	K_F	l/n	R^2
20	0.0596	0.821	4.866	0.628	0.238	1.427	0.995
25	0.0606	0.836	4.640	0.625	0.216	.1464	0.998
30	0.0610	0.840	4.578	0.621	0.213	1.467	0.998
35	0.0615	0.831	4.468	0.619	0.209	1.478	0.998
40	0.0622	0.825	4.359	0.616	0.205	1.486	0.998

(DKR)				Temkin		
β	q_{max}	E	R^2	K_T	B	R^2
-1.5296	4.616	0.571	0.831	0.540	3.285	0.880
-1.5192	4.568	0.573	0.826	0.522	3.314	0.860
-1.5170	4.558	0.574	0.825	0.520	3.315	0.859
-1.5190	4.567	0.573	0.827	0.517	3.326	0.860
-1.5209	4.576	0.573	0.830	0.514	3.332	0.860

As presented in Table (4), the adsorption of Eosin dye on ZnO nanoparticles was fit to Freundlich isotherm by higher correlation factor (R^2) values. The results show what is otherwise based on the correlation coefficient data [30].

The values of dimensionless sorption factor (R_L) were close to zero and this indication for favorable adsorption. The intensity of adsorption (n) showed low values **(**n<1); this indicates a very low affinity between adsorbents and adsorbate [26]. The Freundlich constant (K_F) decreases with increasing the temperature and this indication for exothermic reaction. In isotherm Dubinin (DKR), the energy equation gives us a perception of the adsorption mechanism. (E <8 KJ /mol) indicates that the physical force influence adsorption and that (E>

16) indicates the spread of molecules and when (E) is between (8-16) indicates that adsorption is directed by ion exchange, and the values of (B) less than (40 kJ/mol) this indication for physical adsorption [19].

Thermodynamics parameters

The thermodynamics parameters (ΔH°, ΔG°,Δ S°) of the removal of dye on ZnO were calculated according to the following relations:

$$K_c = Ae^{-\Delta H/RT+\Delta S/R} \quad (13)$$

$$\ln X_m = -\frac{\Delta H}{RT} + C \quad (14)$$

Where ln X_m is the natural logarithm for greatest amount adsorbed (mg/g), K is the constant of Van't Hoff equation, R is the universal gas constant (8.314.10-3 Jmol-1. K-1) and T is the

$$\Delta G^\circ = -RT\ln K \quad (15)$$

$$K = \frac{Q_e \times m}{C_e \times V}$$

$$\Delta G^\circ = \Delta H - T\Delta S^\circ \quad (16)$$

The value ΔH° was calculated from the slope of the Van't Hoff plots (the plots of ln Xm versus 1/T) (Figure (16)) and listed in Table (5) [31]. The value of ΔH° was negative, indicating that the sorption reactions is exothermic. The negative value of ΔS° confirmed the decreased randomness as solid/solution interface during the adsorption process [19]. Gibb's free energy values were negative indicates that the adsorption process was spontaneous and thermodynamically favorable [32].

Table 5: Values of thermodynamic functions for adsorption Eosin dye on (ZnO) nanoparticles

C_e (mg/L)	Thermodynamic function	Co 20	Co 25	Co 30	Co 35	Co 40
20 mg/ L	ΔH kJ.mo^{-1}	-0.144				
	ΔG kJ.mol^{-1}	-5.033	-5.116	-5.197	-5.281	-5.447
	ΔS J.mol^{-1} K^{-1}	0.016686	0.016684	0.016676	0.016678	0.016676

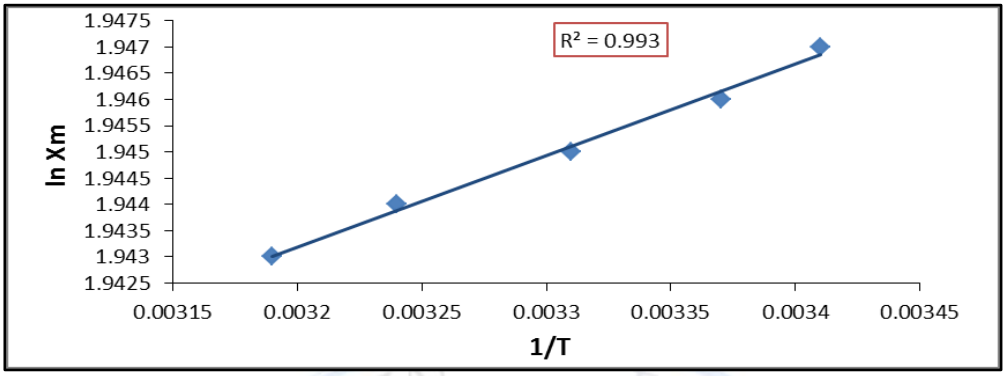

Figure 16: Values of greatest amounts adsorbed (ln X_m) for Eosin dye on (ZnO) nanoparticles at different temperatures (293-318 K).

Conclusions

Based upon the experimental conclusion of this research prove that nano-CuO can be considered as an adsorbent for the treating of Eosin dye from waste water. In installment experimental, the influence of temperature, contact time, initial dye concentration and amount of CuO were show to be effective.

The removal of dye is an exothermic process. It was found that the pseudo – second order model might have followed by the adsorption process as supported by correlation coefficients of the linear plots, and also q_{cala} were very close to the q_{exp} for the pseudo – second order rate kinetics .The isotherm study indicates four isotherms models. Adsorption data was proper to Freundlich isotherm, the Freundlich constant (k_F) decreases with increasing the temperature and this indication for exothermic. In isotherm Dubinin (DKR), the energy equation gives us a perception of the adsorption mechanism. (E <8 KJ /mol) indicates that the physical force influence.

References

1. Li, Y. H.; Liu, T.; Du, Q.; Sun, J.; Xia, Y.; Wang, Z.; Zhang, W.; Wang, K.; Zhu, H.; Wu, D. Chemical and biochemical engineering quarterly 2012, 25 (4), 483-491
2. Reddy, S. S.; Kotaiah, B.; REDDY, N. S. P.; VELU, M. Turkish Journal of Engineering and Environmental Sciences 2007, 30 (6), 367-373.

3. Wang, L.; Zhang, J.; Zhao, R.; Li, C.; Li, Y.; Zhang, C. Desalination 2010, 254 (1-3), 68-74.

4. Kalyani, D. C.; Telke, A. A.; Dhanve, R. S.; Jadhav, J. P. Journal of Hazardous Materials 2009, 163 (2-3), 735-742.

5. Ghoneim, M. M.; El-Desoky, H. S.; Zidan, N. M. Desalination 2011, 274 (1-3), 22-30.

6. Deriszadeh, A. L. I.; Husein, M. M.; Harding, T. G. Environmental science & technology 2010, 44 (5), 1767-1772.

7. Luo, P.; Zhao, Y.; Zhang, B.; Liu, J.; Yang, Y.; Liu, J. Water research 2010, 44 (5), 1489-1497.

8. Meshko, V.; Markovska, L.; Mincheva, M.; Rodrigues, A. E. Water research 2001, 35(14), 3357-3366.

9. Doğan, M.; Alkan, M. Chemosphere 2003, 50 (4), 517-528.

10. Mckay, G. B. H. S.; Blair, H. S.; Gardner, J. R. Journal of applied polymer science 1982, 27 (8), 3043-3057.

11. Kumar, K. V. Dyes and Pigments 2007, 74 (3), 595-597.

12. Chia, C. H.; Razali, N. F.; Sajab, M. S.; Zakaria, S.; Huang, N. M.; Lim, H. N. Sains Malaysiana 2013, 42 (6), 819-826.

13. Smaranda, C.; Gavrilescu, M.; Bulgariu, D. International Journal of Environmental Research 2011, 5 (1), 177-188.

14. Kumar, H.; Rani, R. International Letters of Chemistry, Physics and Astronomy 2013, 14, 26-36.

15. Jing, L.; Xu, Z.; Shang, J.; Sun, X.; Cai, W.; Guo, H. Materials Science and Engineering 2002, A, 332 (1-2), 356-361.

16. Mubarak, T. H.; Hassan, K. H.; Abbas, Z. M. A. In Advanced Materials Research. Trans Tech Publications 2013, 685,119-122.

17. Liu, M.; Dong, F.; Kang, W.; Sun, S.; Wei, H.; Zhang, W.; Nie, X.; Guo, Y.; Huang, T.; Liu, Y. International journal of environmental research and public health 2014, 11(6), 6099-6118.

18. Smaranda, C.; Gavrilescu, M.; Bulgariu, D. International Journal of Environmental

Research 2011, 5(1), 177-188.

19. Amir, F. Dawood; Abd, A. Khudheir, A.; Marwa, I. Mubarak, Diyala University - College of Science 2017, 13 (1), 22-41.

20. Lagergren, S. K. Sven. Vetenskapsakad. Handingarl 1898, 24, 1-39.

21. Ho, Y. S.; McKay, G. Process biochemistry 1999, 34 (5), 451-465.

22. Chia, C. H.; Razali, N. F.; Sajab, M. S.; Zakaria, S.; Huang, N. M.; Lim, H. N. Sains Malaysiana 2013, 42 (6), 819-826.

23. Hassan, K. H.; Mahdi, E. R. Diyala Journal for Pure Science 2017, 13 (2-part 2), 217-234.

24. Ma, J.; Guo, H.; Lei, M.; Wan, X.; Zhang, H.; Feng, X.; Wei, R.; Tian, L.; Han, X. Environmental pollution 2016, 213, 638-647.

25. Crosby, D. G. Environmental transport. Environmental toxicology and chemistry. Oxford University Press, New York, 1998, 51-67.

26. Gan, S.; Zakaria, S.; Chia, C. H.; Chen, R. S.; Jeyalaldeen, N. Cellulose 2015, 22 (6), 3851-3863.

27. Fungaro, D. A.; Yamaura, M.; Carvalho, T. E. M. Journal of Atomic and Molecular Sciences 2011, 2 (4), 305-316.

28. Stoeckli, F. (1998). Recent developments in Dubinin's theory. Carbon, 36 (4), 363-368.

29. Mall, I. D.; Srivastava, V. C.; Agarwal, N. K. Dyes and pigments 2006, 69 (3), 210-223.

30. Farghali, A. A.; Bahgat, M.; Allah, A. E.; Khedr, M. H. Beni-Suef University Journal of Basic and Applied Sciences 2013, 2 (2), 61-71.

31. Haciyakupoglu, S.; Orucoglu, E.; Esen, A. N.; Yusan, S.; Erenturk, S. Desalination and Water Treatment 2015, 56 (5), 1208-1216.

32. Srivastava, V. C.; Swamy, M. M.; Mall, I. D.; Prasad, B.; Mishra, I. M. Colloids and surfaces a: physicochemical and engineering aspects 2006, 272 (1-2), 89-104.